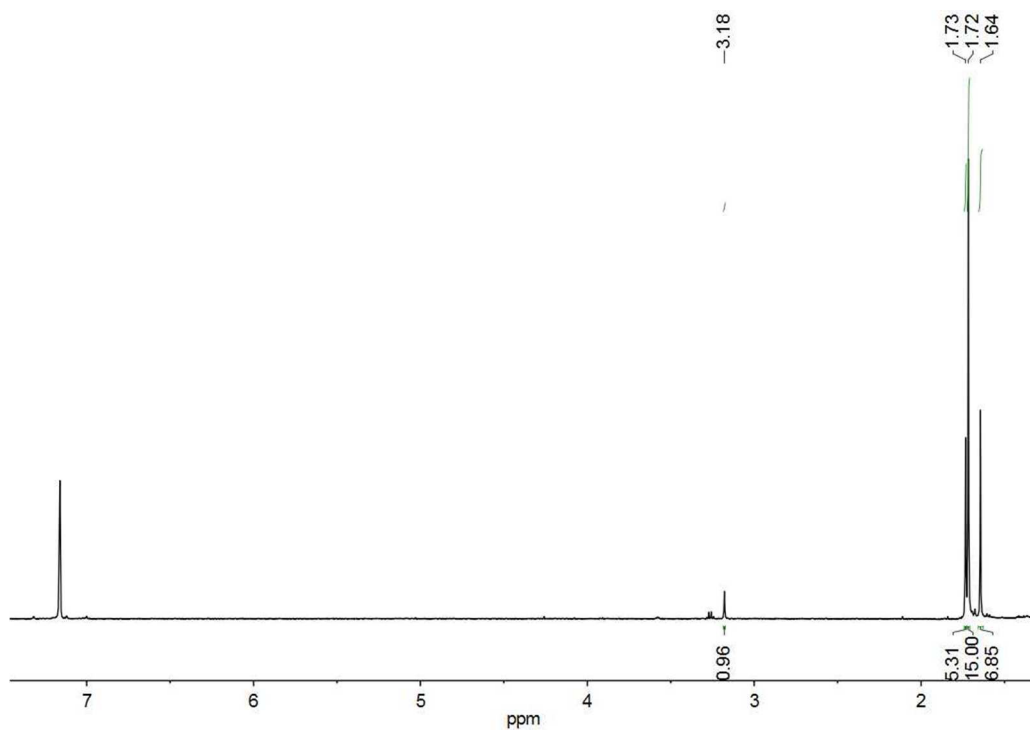


Supporting Information for  
**Hydrogen Production Catalyzed by Bidirectional, Biomimetic Models of the [FeFe]-  
 Hydrogenase Active Site**

James C. Lansing, James M. Camara, Danielle Gray, Thomas B. Rauchfuss\*

***Contents:***

- pS2. Figure S1.  $^1\text{H}$  NMR spectrum of  $\text{FcMe}_9$   
 pS2. Figure S2. CV of  $\text{FcMe}_9$   
 pS3. Figure S3.  $^{31}\text{P}\{^1\text{H}\}$  NMR spectrum of  $[\text{Fe}(\text{C}_5\text{Me}_5)(\text{C}_5\text{Me}_4\text{CH}_2\text{P}^{\text{Et}_2}\text{H})]^+$   
 pS3. Figure S4.  $^1\text{H}$  NMR spectrum of  $[\text{Fe}(\text{C}_5\text{Me}_5)(\text{C}_5\text{Me}_4\text{CH}_2\text{P}^{\text{Et}_2}\text{H})]^+$   
 pS4. Figure S5.  $^1\text{H}$  NMR spectrum of  $\text{PFc}^{\#\text{Et}_2}$   
 pS4. Figure S6.  $^{31}\text{P}\{^1\text{H}\}$  NMR spectrum of  $\text{FcP}^{\#\text{Et}_2}$   
 pS5. Figure S7. CV of  $\text{PFc}^{\#\text{Et}_2}$   
 pS5. Figure S8. CV of  $\text{PFc}^{\#\text{Et}_2}$   
 pS6. Figure S9.  $^1\text{H}$  NMR of  $\text{PFc}^{\#\text{Cy}_2}$   
 pS6. Figure S10.  $^{31}\text{P}\{^1\text{H}\}$  NMR spectrum of  $\text{PFc}^{\#\text{Cy}_2}$   
 pS7. Figure S11. CV of  $\text{PFc}^{\#\text{Cy}_2}$   
 pS7. Figure S12. CV of  $\text{PFc}^{\#\text{Cy}_2}$   
 pS8. Figure S13.  $^1\text{H}$  NMR spectrum of  $\text{PFc}^{\#\text{Ph}_2}$   
 pS8. Figure S14.  $^{31}\text{P}\{^1\text{H}\}$  NMR spectrum of  $\text{PFc}^{\#\text{Ph}_2}$   
 pS9. Figure S15. CV of  $\text{PFc}^{\#\text{Ph}_2}$   
 pS9. Figure S16. CV of  $\text{PFc}^{\#\text{Ph}_2}$   
 pS10. Figure S17.  $^1\text{H}$  NMR spectrum of  $\text{Fe}_2(\text{adt}^{\text{Bn}})(\text{CO})_3(\text{dppv})(\text{PFc}^{\#\text{Et}_2})$   
 pS10. Figure S18.  $^{31}\text{P}\{^1\text{H}\}$  NMR spectrum of  $\text{Fe}_2(\text{adt}^{\text{Bn}})(\text{CO})_3(\text{dppv})(\text{PFc}^{\#\text{Et}_2})$   
 pS11. Figure S19. CV of  $\text{Fe}_2(\text{adt}^{\text{Bn}})(\text{CO})_3(\text{dppv})(\text{PFc}^{\#\text{Et}_2})$   
 pS11. Figure S20.  $^1\text{H}$  NMR spectrum of  $\text{Fe}_2(\text{pdt})(\text{CO})_3(\text{dppv})(\text{PFc}^{\#\text{Et}_2})$   
 pS12. Figure S21.  $^{31}\text{P}\{^1\text{H}\}$  NMR spectrum of  $\text{Fe}_2(\text{pdt})(\text{CO})_3(\text{dppv})(\text{PFc}^{\#\text{Et}_2})$   
 pS12. Figure S22. CV of  $\text{Fe}_2(\text{pdt})(\text{CO})_3(\text{dppv})(\text{PFc}^{\#\text{Et}_2})$   
 pS13. Figure S23. Tautomerization of  $[\text{H1}]^+$  to form  $[\text{1H}]^+$  monitored by IR  
 pS14. Figure S24. Kinetic plot of the tautomerization of  $[\text{H1}]^+$  to form  $[\text{1H}]^+$   
 pS14. Figure S25. IR of **1** with >2 equiv of  $[\text{H}(\text{OEt}_2)_2]\text{BAr}^{\text{F}}_4$   
 pS15. Figure S26. IR spectrum 2.5 h after catalytic HER with **2**  
 pS15. Figure S27. IR spectrum from Figure 8 at 2nd time point  
 pS16. Figure S28. IR spectrum from Figure 8 at 3rd time point  
 pS16. Figure S29. IR spectrum from Figure 8 at 4th time point  
 pS17. Figure S30. Protonation and subsequent oxidation of  $[\text{1}]^+$   
 pS18. Figure S31.  $^{31}\text{P}\{^1\text{H}\}$  NMR spectrum of  $\text{Fe}_2(\text{adt}^{\text{Bn}})(\text{CO})_3(\text{dppv})(\text{PMe}_3) + [\text{H}(\text{OEt}_2)_2]\text{BAr}^{\text{F}}_4$ .  
 pS19. Figure S32. IR spectra for reaction of **1** +  $[\text{NPh}_2\text{H}_2]\text{BAr}^{\text{F}}_4$ .



**Figure S1.** <sup>1</sup>H NMR spectrum of FcMe<sub>9</sub> in C<sub>6</sub>D<sub>6</sub> solution.

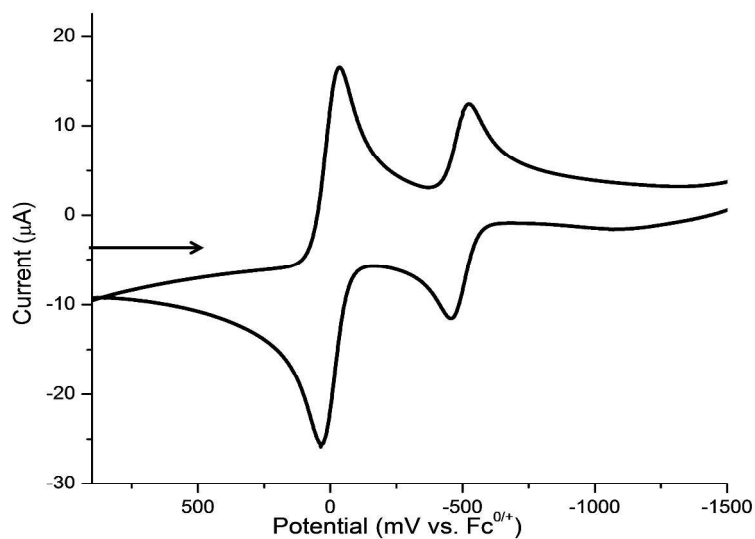


**Figure S2.** Cyclic voltammogram of 1.0 mM FcMe<sub>9</sub> in CH<sub>2</sub>Cl<sub>2</sub> solution at 25 °C at 0.05 V/s.  $E_{1/2} = -490$  mV ( $i_{pa}/i_{pc} = 0.88$ ). Conditions: 0.1 M [Bu<sub>4</sub>N]PF<sub>6</sub> supporting electrolyte, Pt working and counter electrodes, Ag wire pseudoreference electrode. FeCp<sub>2</sub> is present as an internal standard.

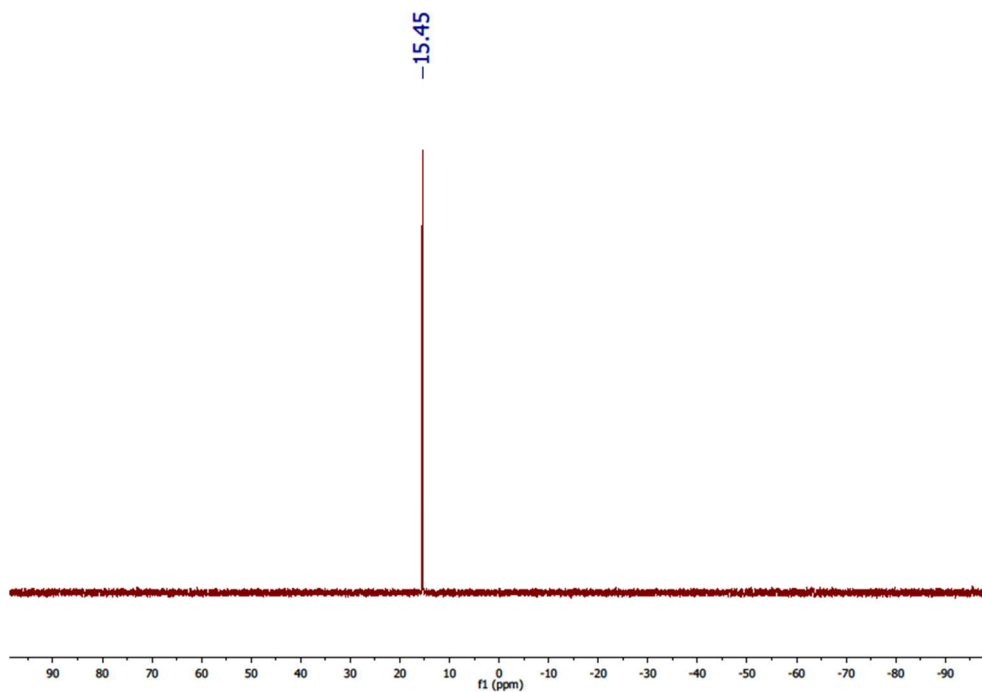


**Figure S3.**  $^{31}\text{P}\{^1\text{H}\}$  NMR spectrum of  $[\text{Fe}(\text{C}_5\text{Me}_5)(\text{C}_5\text{Me}_4\text{CH}_2\text{PEt}_2\text{H})]^+$  in  $\text{CD}_2\text{Cl}_2$  solution.

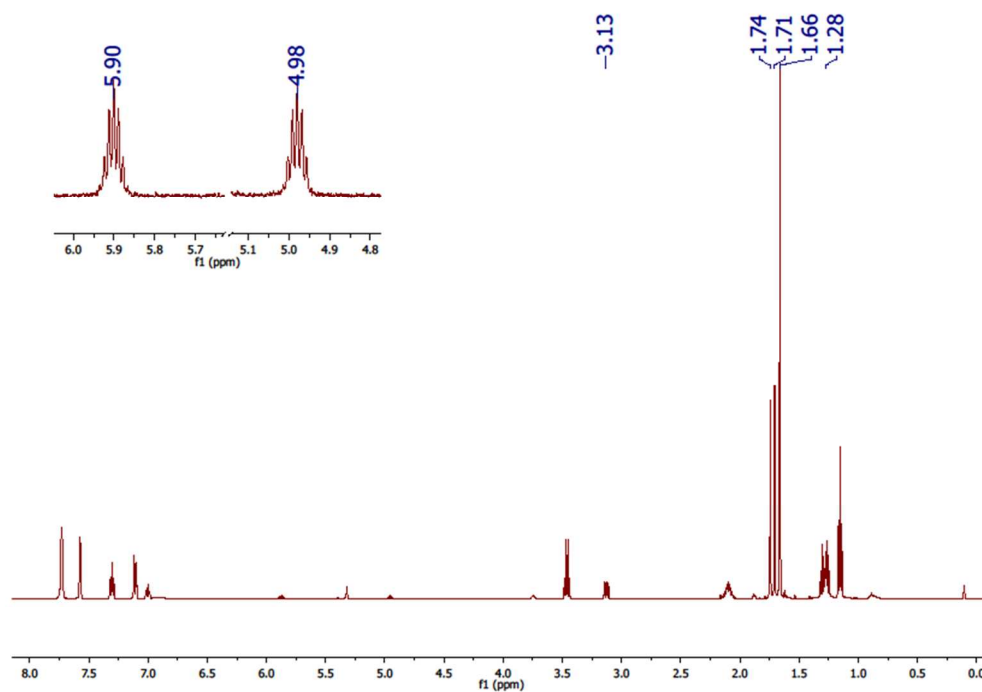


**Figure S4.**  $^1\text{H}$  NMR spectrum of  $[\text{Fe}(\text{C}_5\text{Me}_5)(\text{C}_5\text{Me}_4\text{CH}_2\text{PEt}_2\text{H})]^+$  in  $\text{CD}_2\text{Cl}_2$  solution. Region for the  $\text{PH}$  proton is enhanced.

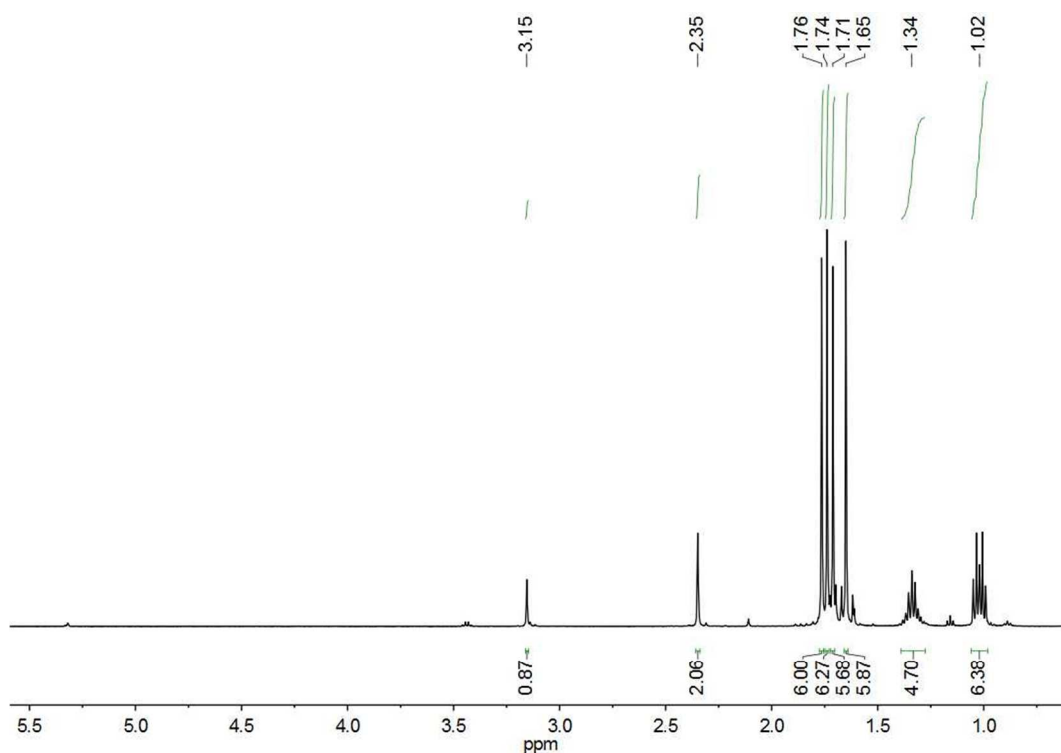


**Figure S5.**  $^1\text{H}$  NMR spectrum of  $\text{PFC}^{\#}\text{Et}_2$  in  $\text{CD}_2\text{Cl}_2$  solution.

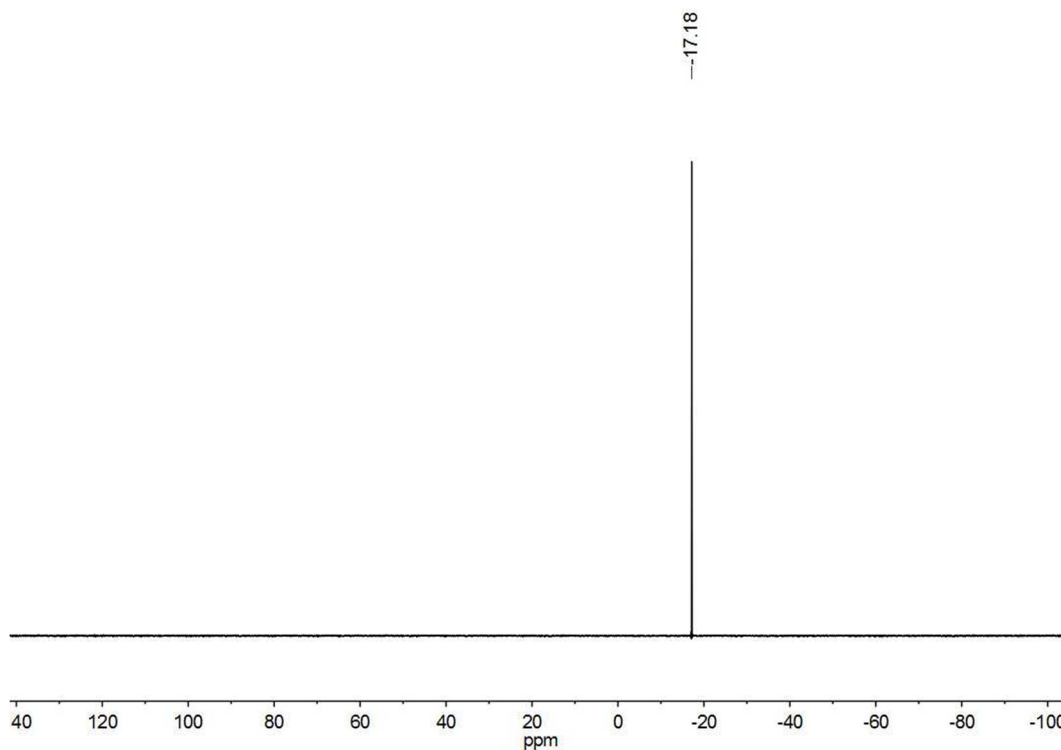


**Figure S6.**  $^{31}\text{P}\{^1\text{H}\}$  NMR spectrum of  $\text{PFC}^{\#}\text{Et}_2$  in  $\text{CD}_2\text{Cl}_2$  solution.

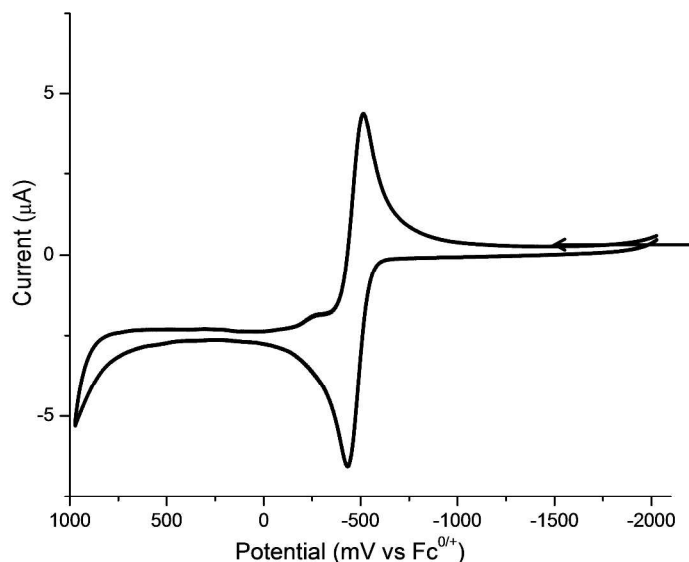


**Figure S7.** Cyclic voltammogram of 1.0 mM  $\text{PFC}^{\#\text{Et}_2}$  in  $\text{CH}_2\text{Cl}_2$  at 25 °C at 0.1 V/s.  $E_{1/2} = -475$  mV ( $i_{\text{pa}}/i_{\text{pc}} = 1.0$ ). Conditions: 0.1 M  $[\text{Bu}_4\text{N}]\text{PF}_6$  supporting electrolyte, Pt working and counter electrodes, Ag wire pseudoreference electrode. Ferrocene (Fc) was added at a later scan as an internal standard.

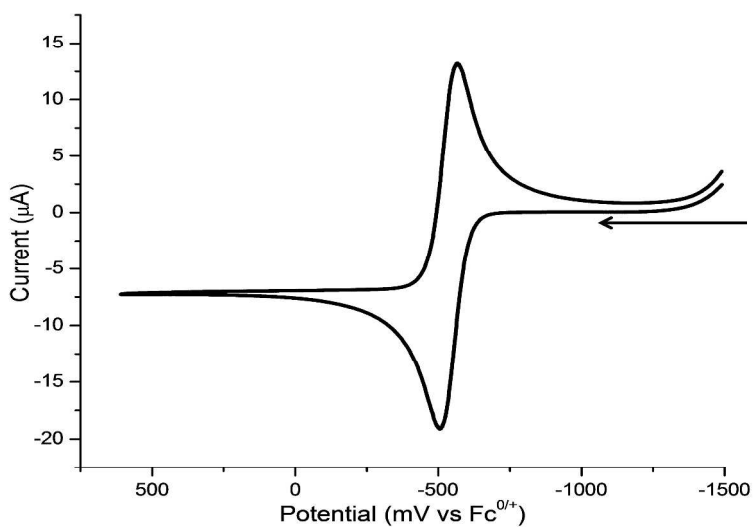


**Figure S8.** Cyclic voltammogram of 1.0 mM  $\text{PFC}^{\#\text{Et}_2}$  in  $\text{CH}_2\text{Cl}_2$  at 25 °C at 0.1 V/s.  $E_{1/2} = -536$  mV ( $i_{\text{pa}}/i_{\text{pc}} = 0.98$ ). Conditions: 0.025 M  $[\text{Bu}_4\text{N}]\text{BAR}_4^{\text{F}}$  supporting electrolyte, Pt working and counter electrodes, Ag wire pseudoreference electrode. Fc was added at a later scan as an internal standard.

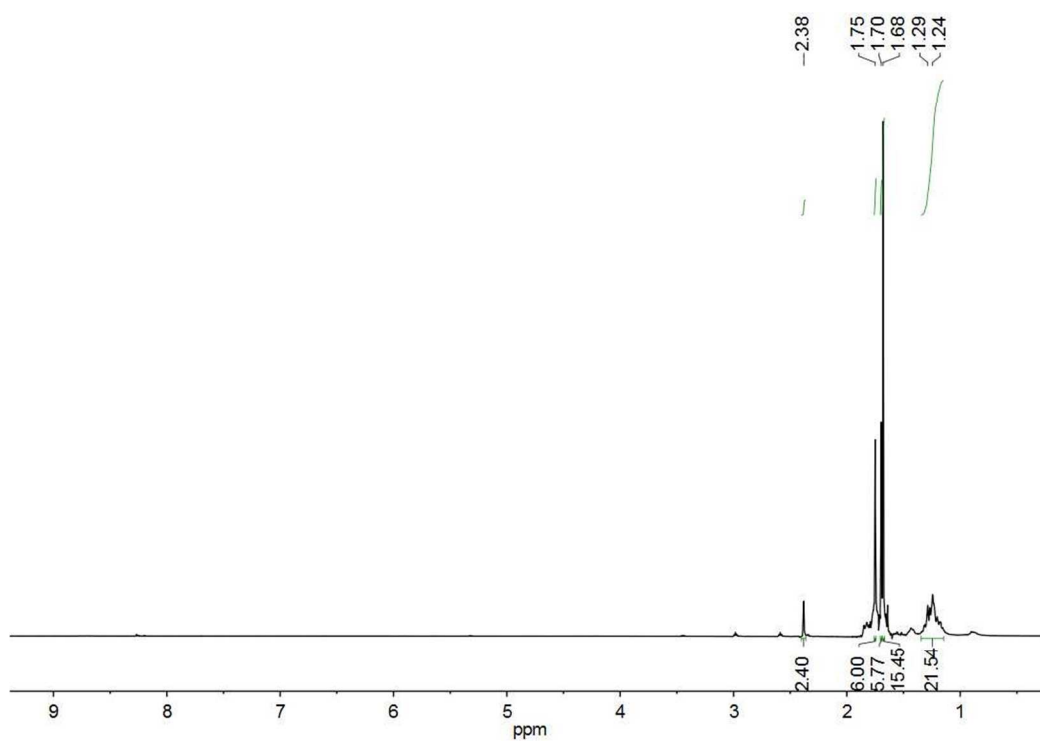


**Figure S9.**  $^1\text{H}$  NMR spectrum of  $\text{PFc}^*\text{Cy}_2$  in  $\text{CD}_2\text{Cl}_2$  solution.

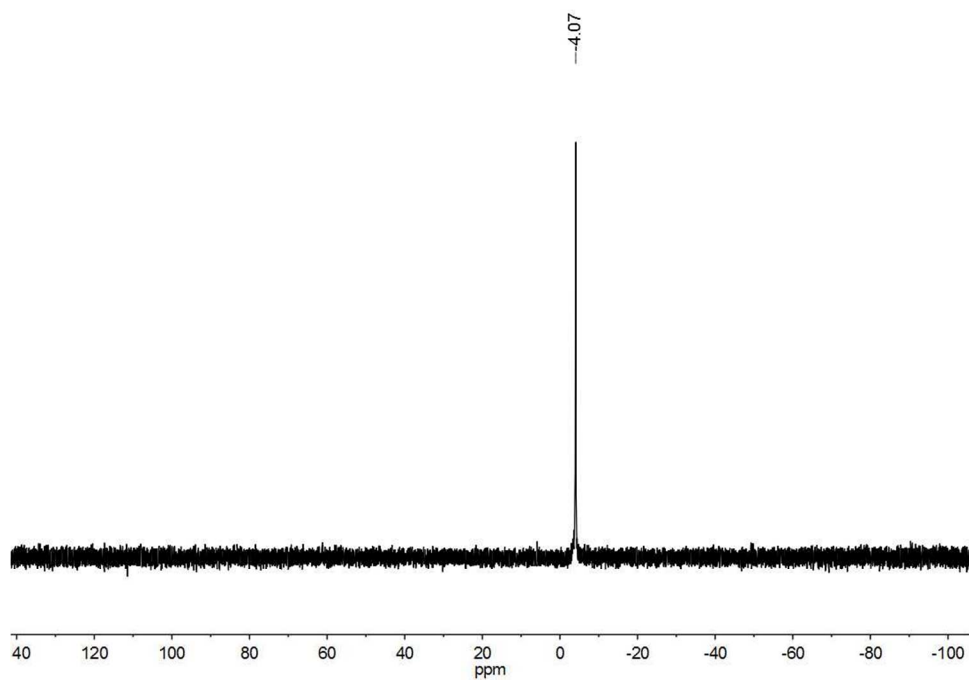


**Figure S10.**  $^{31}\text{P}\{^1\text{H}\}$  NMR spectrum of  $\text{PFc}^*\text{Cy}_2$  in  $\text{CD}_2\text{Cl}_2$  solution.

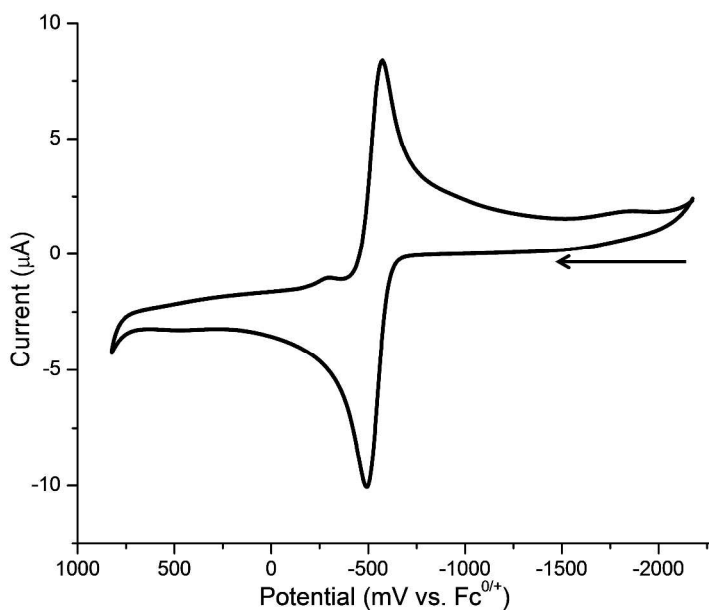


**Figure S11.** Cyclic voltammogram of 1.0 mM PFc\* $\text{Cy}_2$  in  $\text{CH}_2\text{Cl}_2$  at 25 °C at 0.1 V/s in  $[\text{Bu}_4\text{N}]\text{PF}_6$ .  $E_{1/2} = -539$  mV ( $i_{\text{pa}}/i_{\text{pc}} = 0.96$ ). Conditions: see Figure S7.

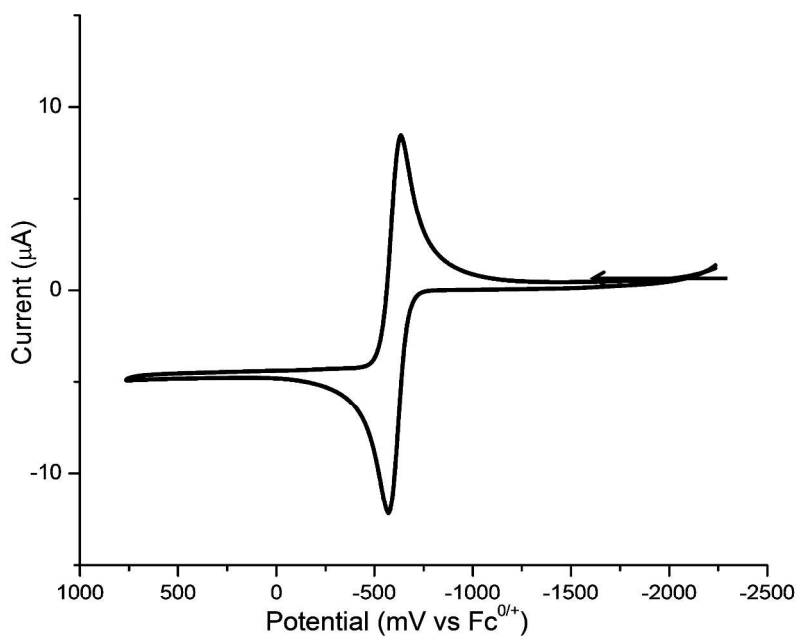


**Figure S12.** Cyclic voltammogram of 1.0 mM PFc\* $\text{Cy}_2$  in  $\text{CH}_2\text{Cl}_2$  solution at 25 °C at 0.1 V/s in  $[\text{Bu}_4\text{N}]\text{BAr}^{\text{F}}_4$ .  $E_{1/2} = -602$  mV ( $i_{\text{pa}}/i_{\text{pc}} = 0.96$ ). Conditions: see Figure S8.

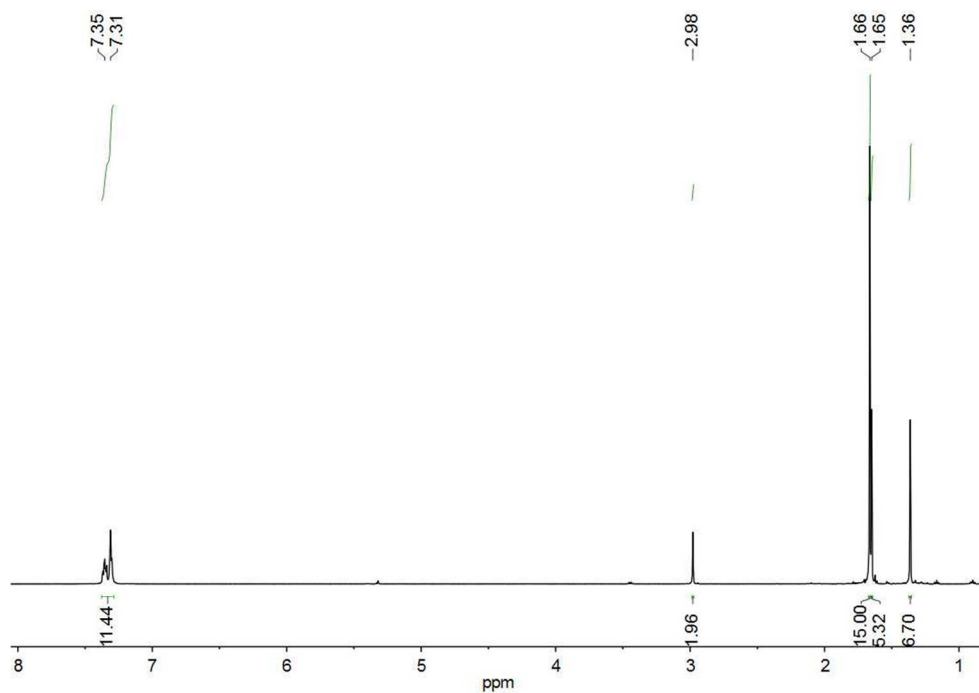


**Figure S13.**  $^1\text{H}$  NMR spectrum of  $\text{PFC}^*\text{Ph}_2$  in  $\text{CD}_2\text{Cl}_2$  solution.

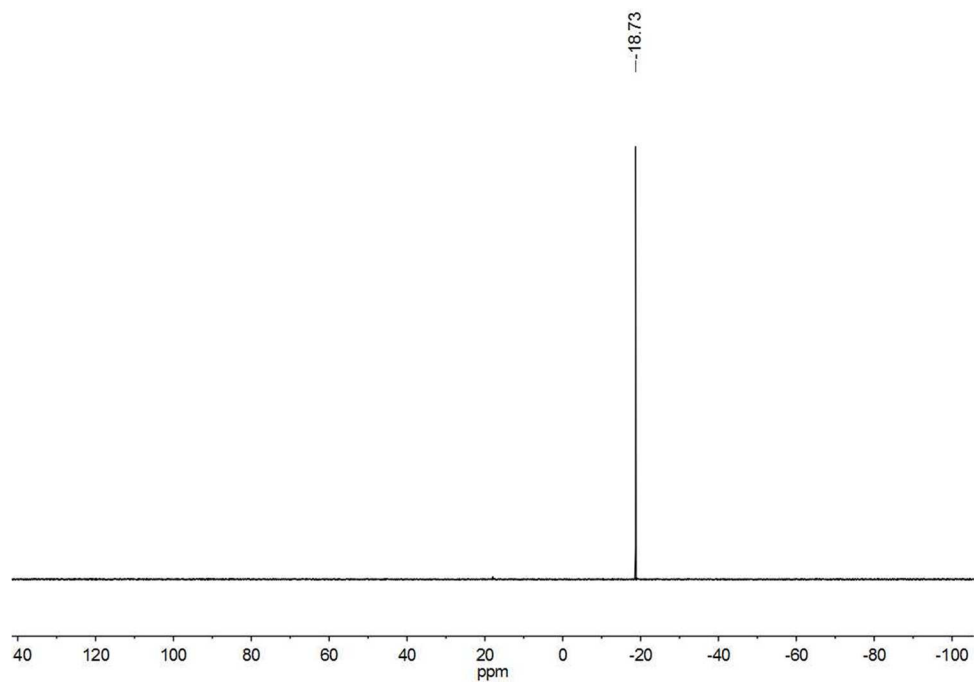


**Figure S14.**  $^{31}\text{P}\{^1\text{H}\}$  NMR spectrum of  $\text{PFC}^*\text{Ph}_2$  in  $\text{CD}_2\text{Cl}_2$  solution.



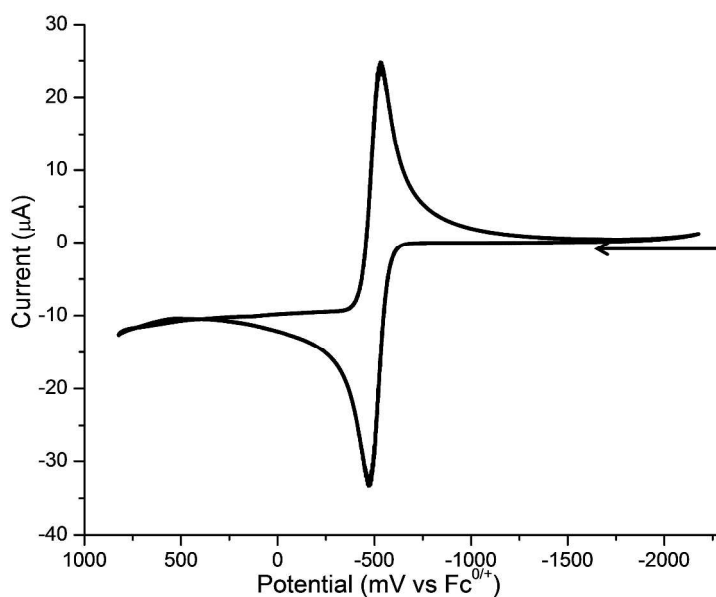


**Figure S15.** Cyclic voltammogram of 1.0 mM PFc\*<sup>Ph<sub>2</sub></sup> in CH<sub>2</sub>Cl<sub>2</sub> at 25 °C at 0.1 V/s in [Bu<sub>4</sub>N]PF<sub>6</sub>.  $E_{1/2} = -501$  mV ( $i_{pa}/i_{pc} = 0.98$ ). Conditions: see Figure S7.

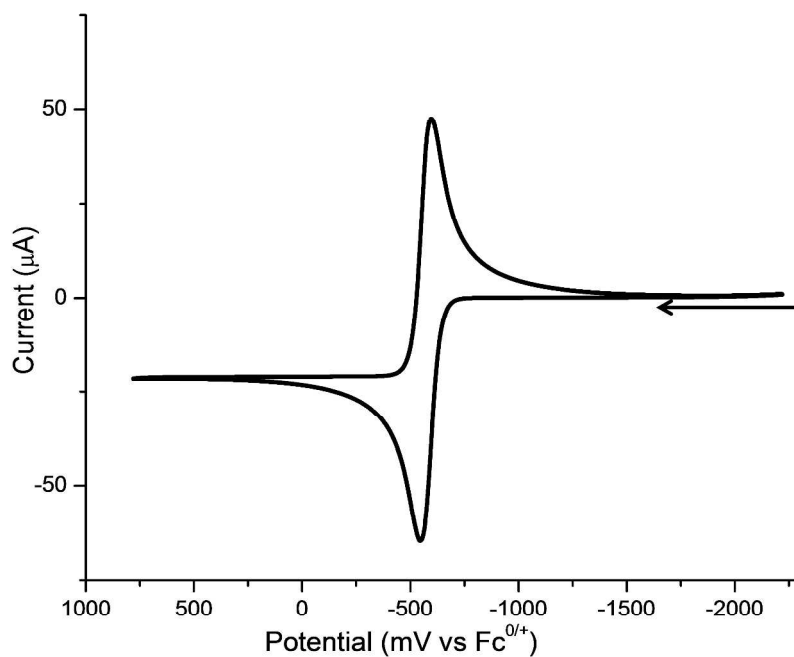


**Figure S16.** Cyclic voltammogram of 1.0 mM PFc\*<sup>Ph<sub>2</sub></sup> in CH<sub>2</sub>Cl<sub>2</sub> solution at 25 °C at 0.1 V/s in [Bu<sub>4</sub>N]BARF<sub>4</sub>.  $E_{1/2} = -572$  mV ( $i_{pa}/i_{pc} = 0.95$ ). Conditions: see Figure S8.

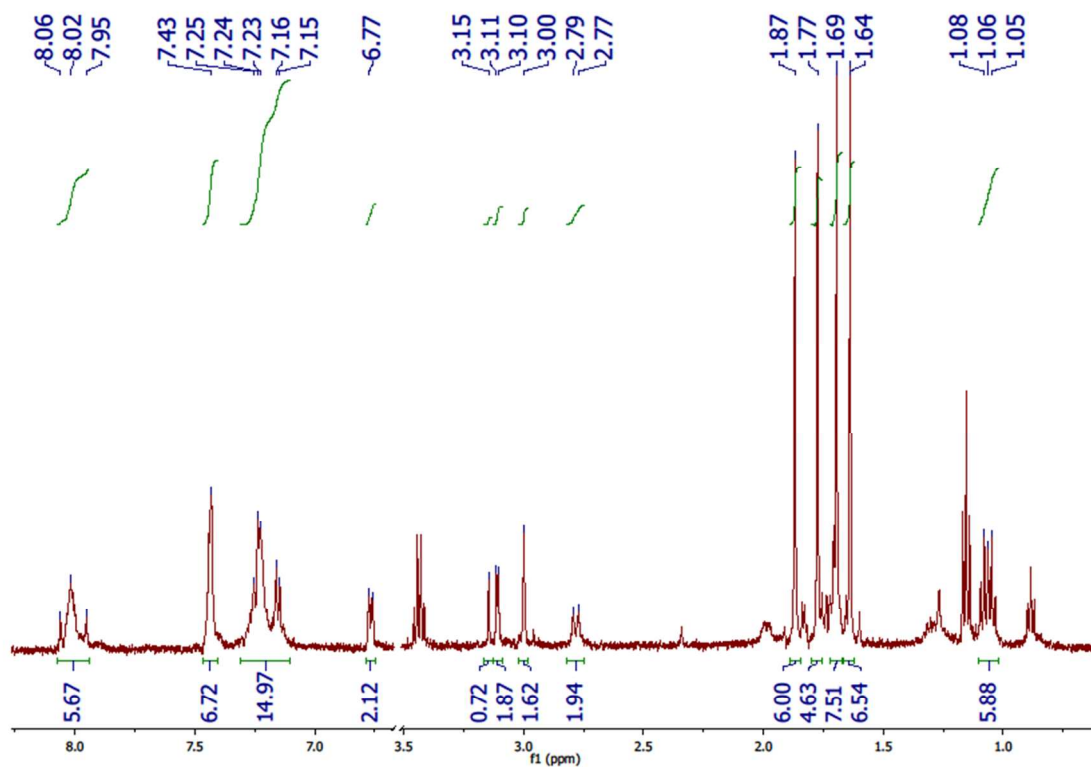


Figure S17.  $^1\text{H}$  NMR spectrum of  $\text{Fe}_2(\text{adt}^{\text{Bn}})(\text{CO})_3(\text{dppv})(\text{PFc}^{\#Et_2})$  in  $\text{CD}_2\text{Cl}_2$  solution.

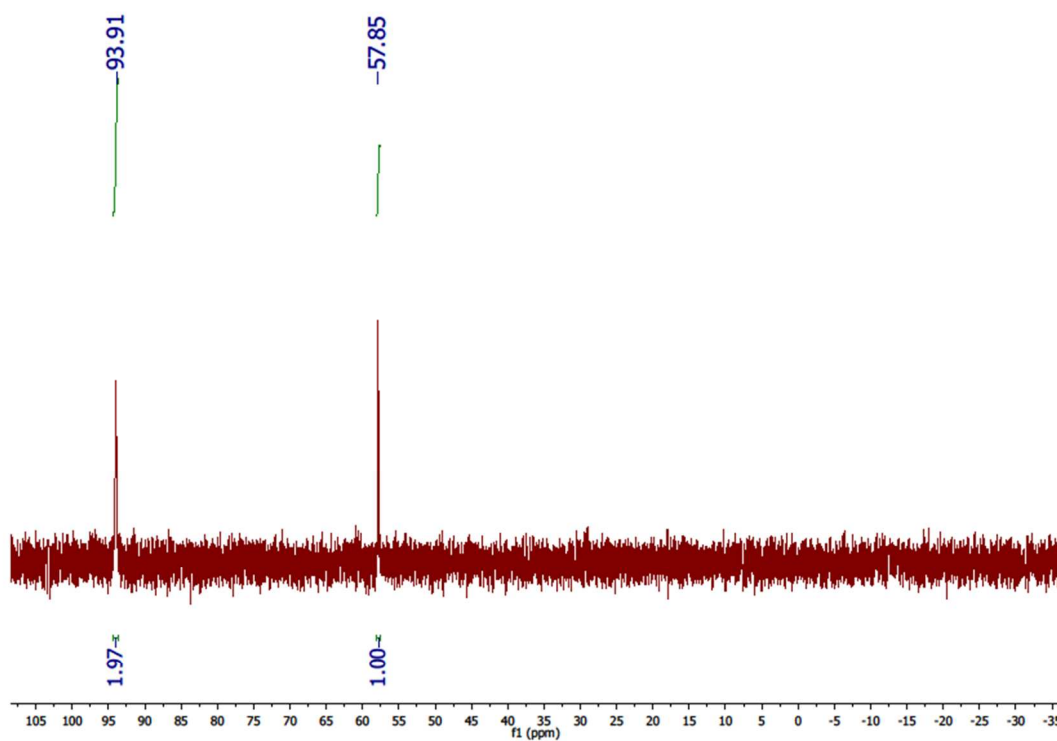
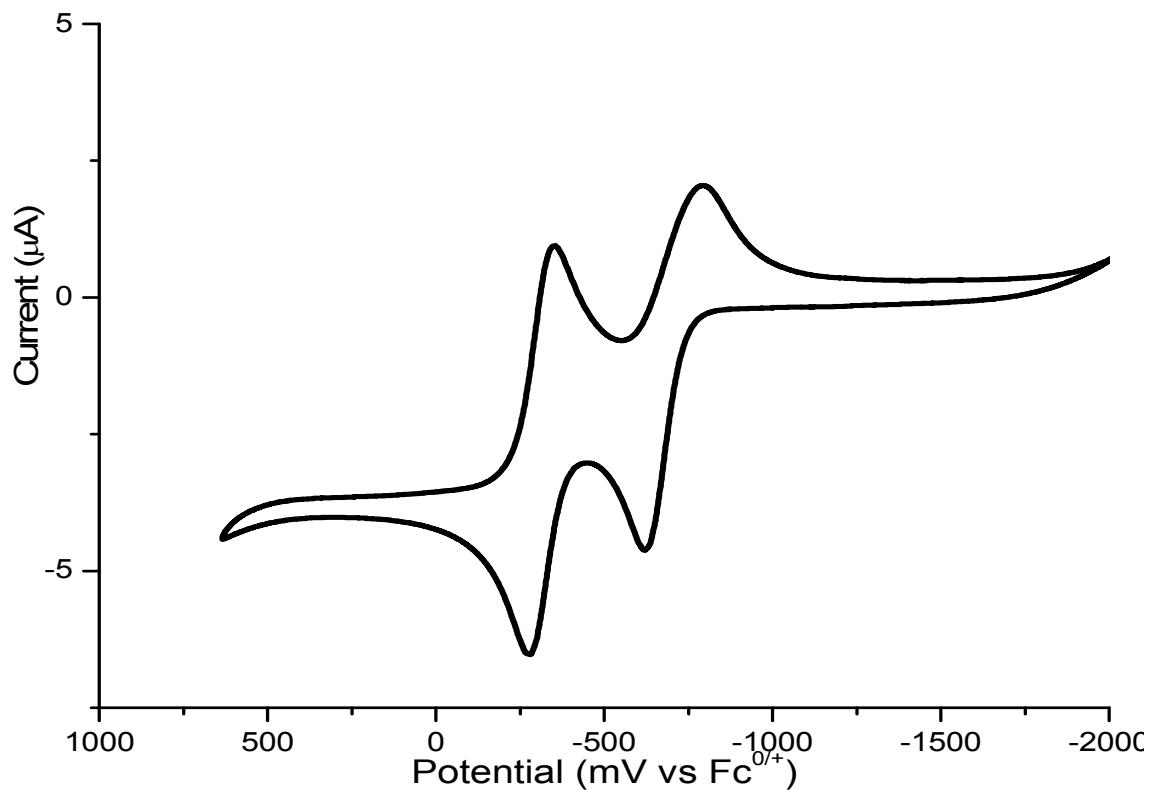
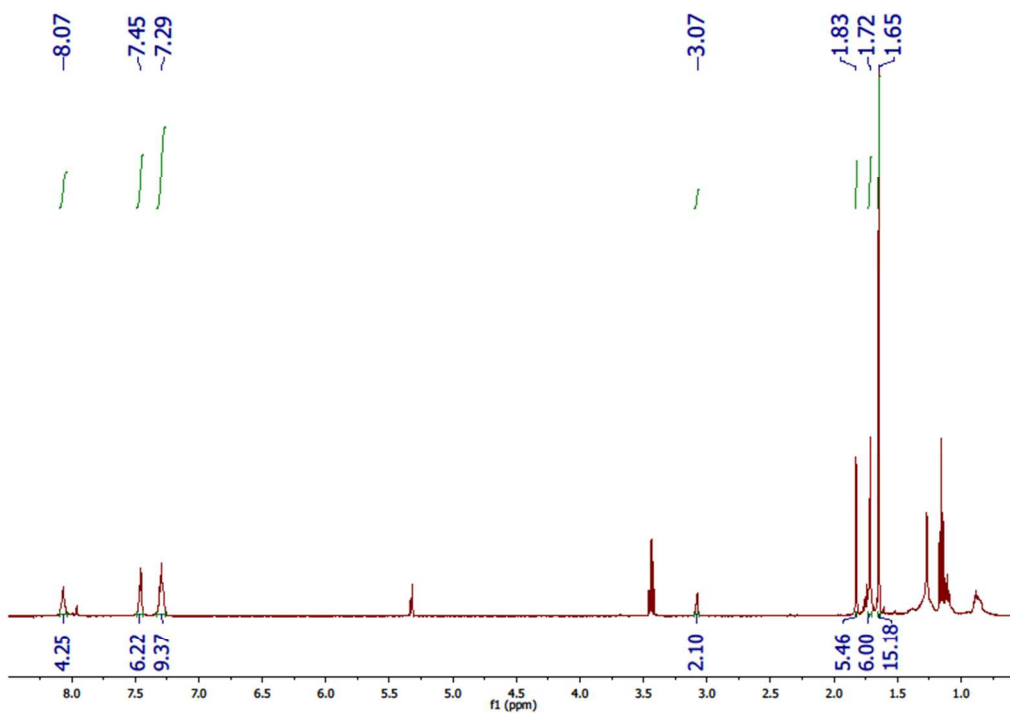


Figure S18.  $^{31}\text{P}\{^1\text{H}\}$  NMR spectrum of  $\text{Fe}_2(\text{adt}^{\text{Bn}})(\text{CO})_3(\text{dppv})(\text{PFc}^{\#Et_2})$  in  $\text{CD}_2\text{Cl}_2$  solution.



**Figure S19.** Cyclic voltammogram of 1.0 mM  $\text{Fe}_2(\text{adt}^{\text{Bn}})(\text{CO})_3(\text{dppv})(\text{PFc}^{\#Et_2})$  in  $\text{CH}_2\text{Cl}_2$  solution at 25 °C at 0.1 V/s in  $[\text{Bu}_4\text{N}]\text{BARF}_4$ .  $E_{1/2} = -713$  mV ( $i_{pa}/i_{pc} = 0.77$ ),  $-315$  mV ( $i_{pa}/i_{pc} = 0.86$ ). Conditions: see Figure S8.



**Figure S20.**  $^1\text{H}$  NMR spectrum of  $\text{Fe}_2(\text{pdt})(\text{CO})_3(\text{dppv})(\text{PFc}^{\#Et_2})$  in  $\text{CD}_2\text{Cl}_2$  solution.

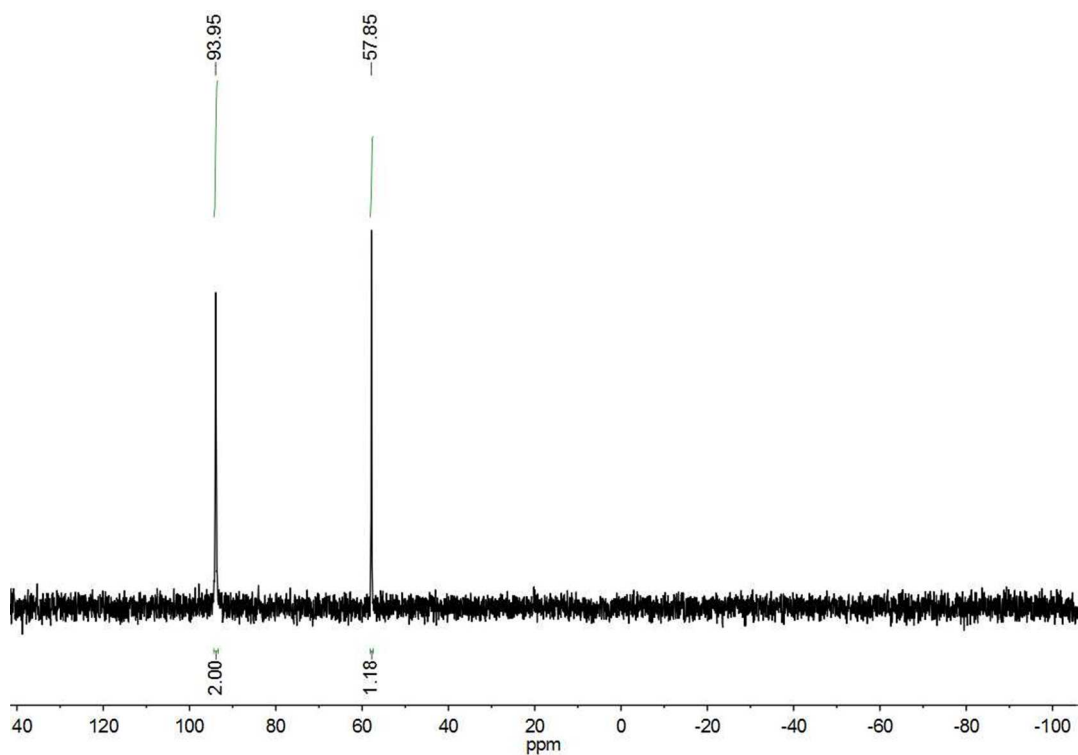


**Figure S21.**  $^{31}\text{P}\{^1\text{H}\}$  NMR spectrum of  $\text{Fe}_2(\text{pdt})(\text{CO})_3(\text{dppv})(\text{PFc}^{\text{Et}_2})$  in  $\text{CD}_2\text{Cl}_2$  solution.

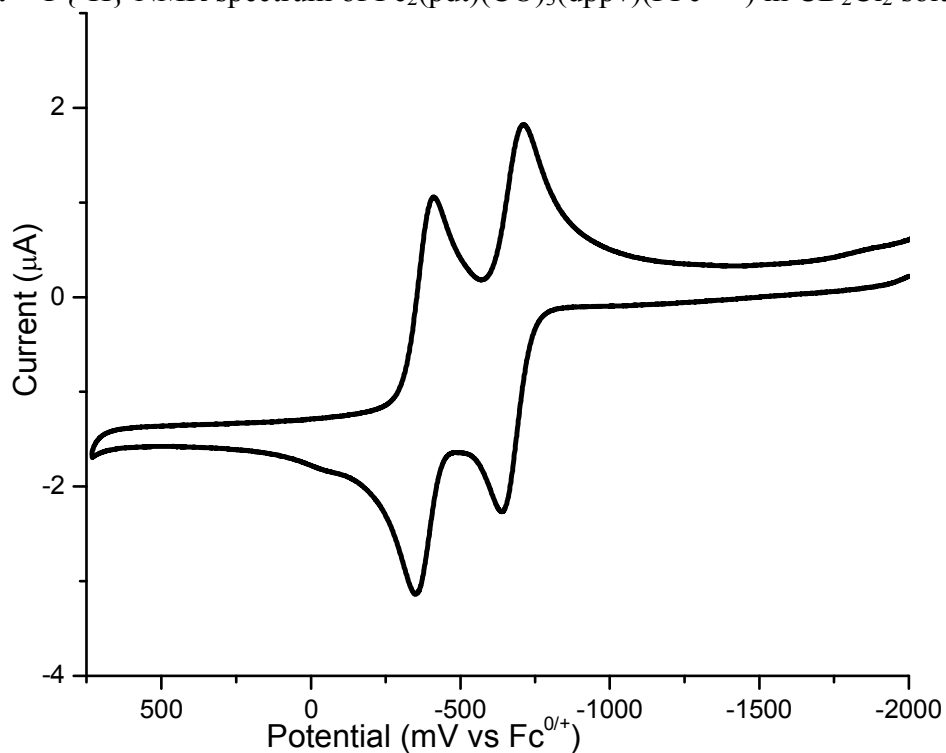


**Figure S22.** Cyclic voltammogram of 1.0 mM of  $\text{Fe}_2(\text{pdt})(\text{CO})_3(\text{dppv})(\text{PFc}^{\text{Et}_2})$  in  $\text{CH}_2\text{Cl}_2$  solution at 25 °C at 0.1 V/s in  $[\text{Bu}_4\text{N}]\text{BARF}_4$ .  $E_{1/2} = -675$  mV ( $i_{\text{pa}}/i_{\text{pc}} = 0.73$ ),  $-382$  mV ( $i_{\text{pa}}/i_{\text{pc}} = 0.97$ ). Conditions: see Figure S8.

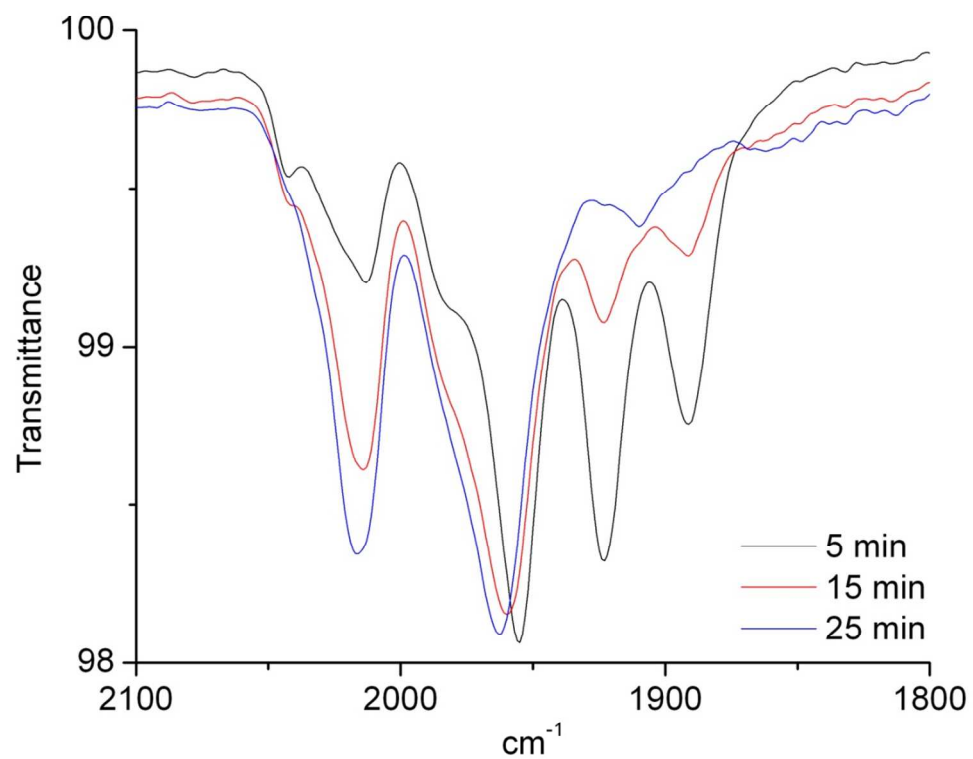


**Figure S23.** Tautomerization of N-protonated [1H]<sup>+</sup> to the hydride [H1]<sup>+</sup> monitored by solution IR spectroscopy (CH<sub>2</sub>Cl<sub>2</sub>, 28 °C).

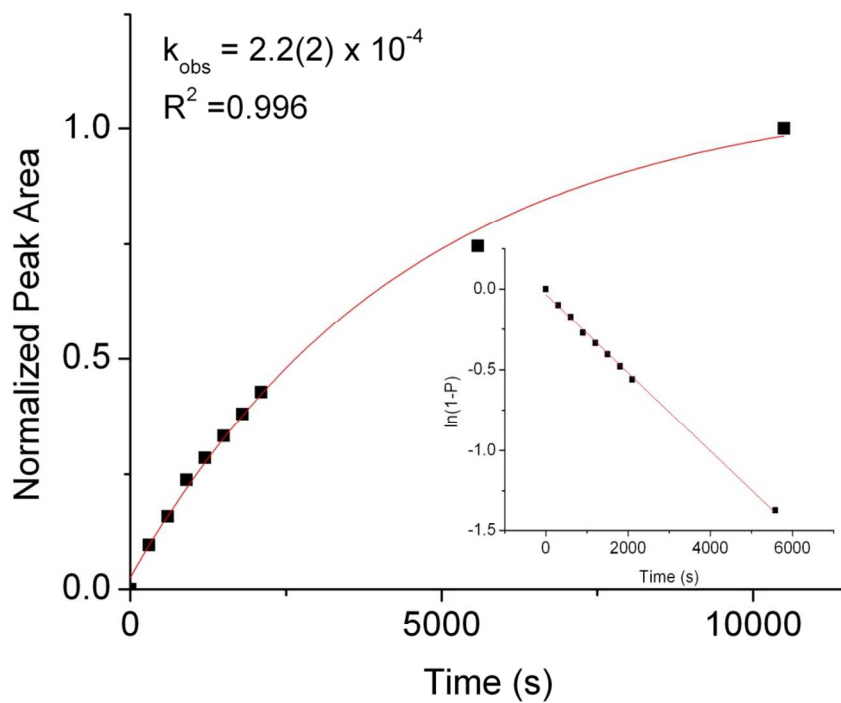


**Figure S24.** Kinetic plot of the tautomerization of N-protonated  $[1H]^+$  to the hydride  $[\mu-H1]^+$ , as monitored by  $^1H$  NMR spectroscopy and fit to a first order exponential. *Inset:* linearized first plot.

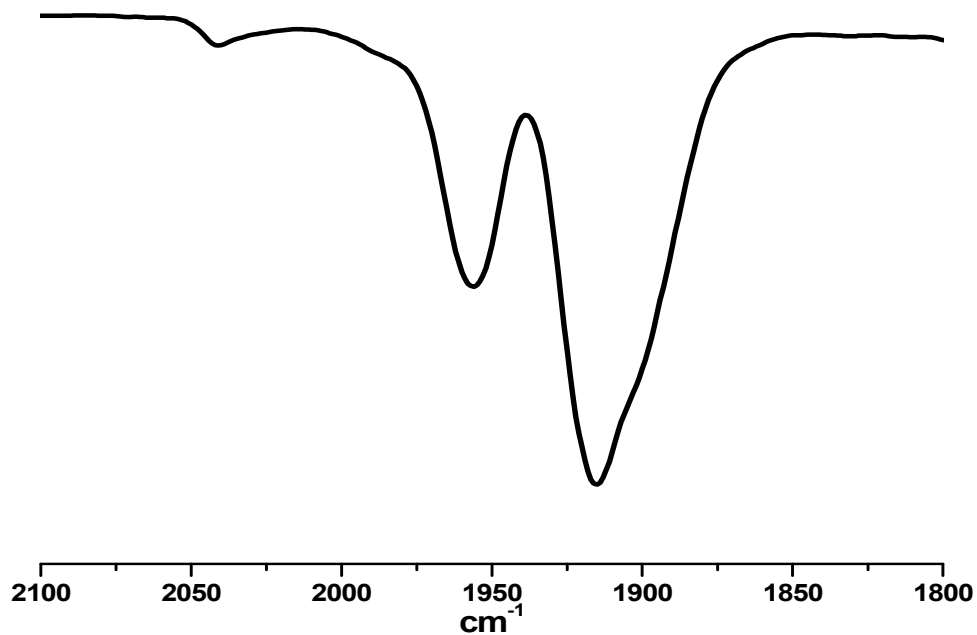


**Figure S25.** IR spectra ( $CH_2Cl_2$  solution) of a solution prepared by treating  $[1]^0$  at  $-15$  °C with  $>2$  equiv of  $[H(OEt_2)_2]BAr^F_4$ .

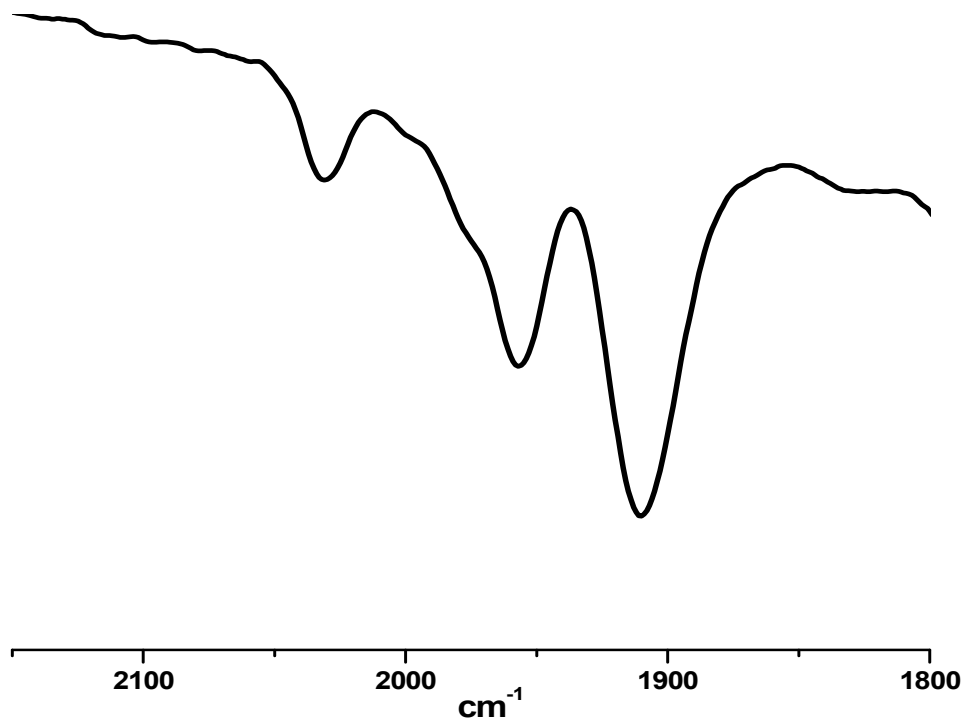


**Figure S26.** IR spectrum 2.5 h after the addition of 5 equiv Fc\* and 10 equiv of  $[\text{H}(\text{OEt}_2)_2]\text{BAr}^{\text{F}_4}$  to  $[\mathbf{2}]^0$ .

*Assignments:*

$[\mathbf{2H}]^{2+}$ : 1957 and 1910  $\text{cm}^{-1}$

$[\mu\text{-H2}]^+$ : 2031  $\text{cm}^{-1}$

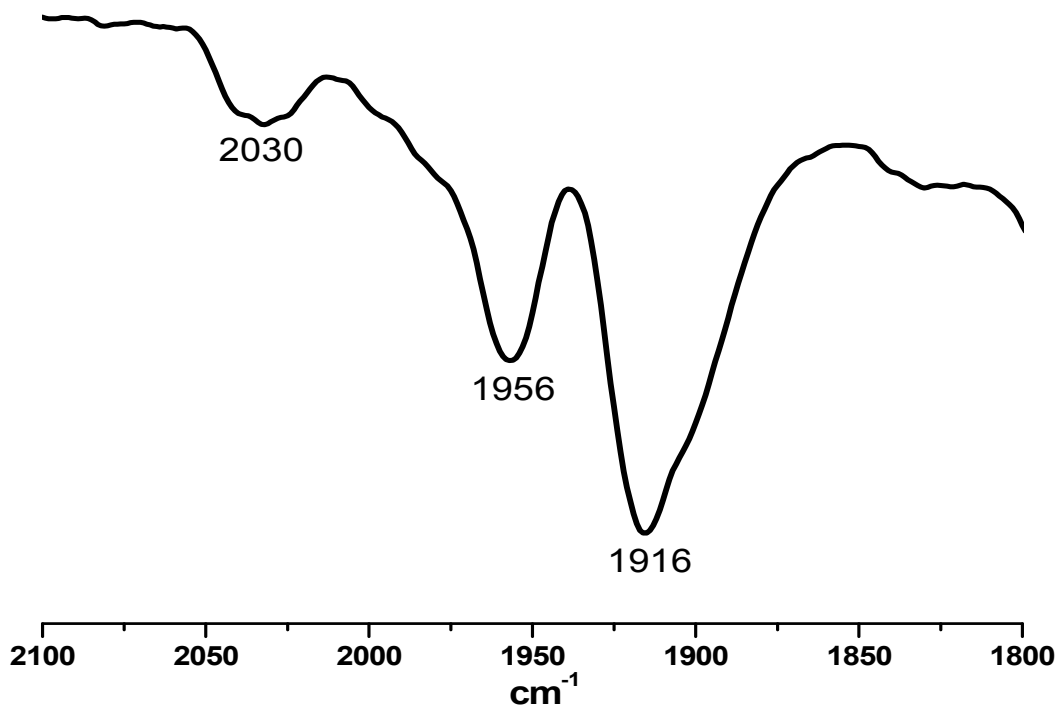


**Figure S27.** IR spectrum of reaction solution at the 2nd time point in Figure 8. Predominant species in solution identified as the ammonium-ferrocenium dication  $[\mathbf{1H}]^{2+}$ .

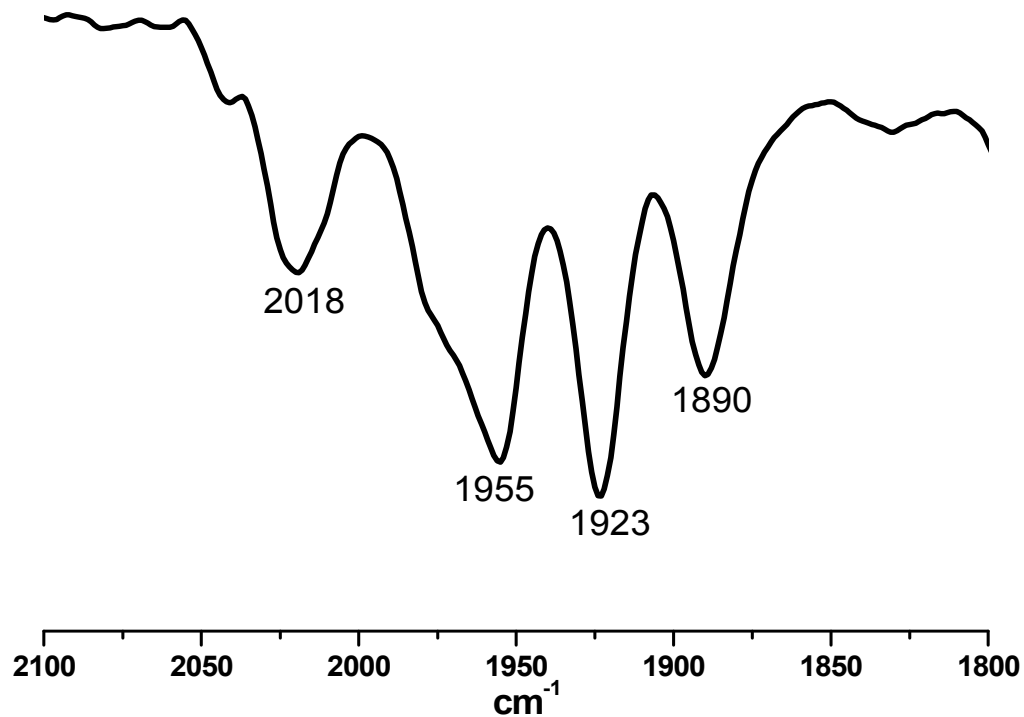


**Figure S28.** IR spectrum of reaction solution at the 3rd time point in Figure 8.

*Assignments:*

$[\text{H1}]^+$ : 1955, 1923, 1890  $\text{cm}^{-1}$

$[\mu\text{-H1}]^+$ : 2018, shoulder near 1970  $\text{cm}^{-1}$

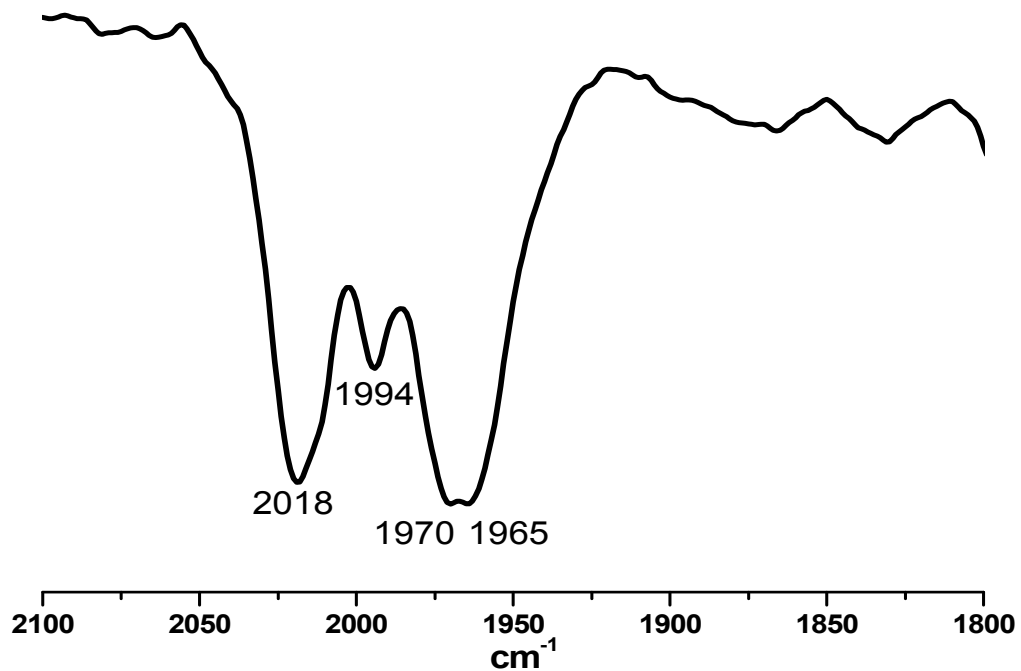


**Figure S29.** IR spectrum of reaction solution at the 4th time point in Figure 8.

*Assignment:*

$[\mu\text{-H1}]^+$ : 2018, 1970  $\text{cm}^{-1}$ .



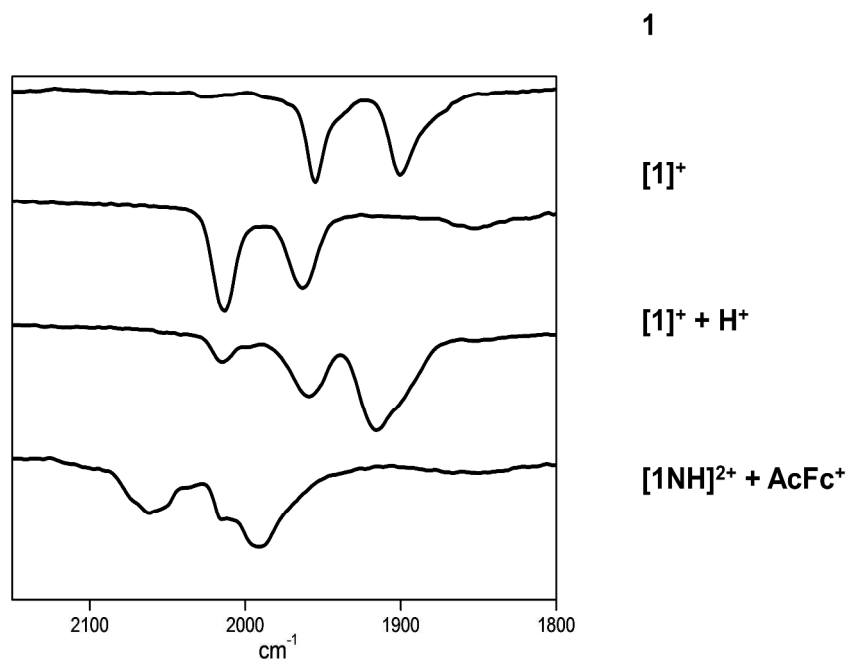


**Figure S30.** IR spectra (CH<sub>2</sub>Cl<sub>2</sub> solutions) for Fe<sub>2</sub>(adt<sup>Bn</sup>)(CO)<sub>3</sub>(dppv)(PFc\*Et<sub>2</sub>) ([1]<sup>0</sup>) (top), the resulting solution after 1.0 equiv of FcBAR<sup>F</sup><sub>4</sub> (middle top), further reaction of [1]<sup>+</sup> with an equiv of [H(OEt<sub>2</sub>)<sub>2</sub>]BAR<sup>F</sup><sub>4</sub> (middle bottom) and the result of addition of 1 equiv of acetylferrocenium to that solution.

*Reference:*

[1]<sup>0</sup>: 1955, 1900 cm<sup>-1</sup>

[1]<sup>+</sup>: 2013, 1963 cm<sup>-1</sup>

[1H]<sup>2+</sup>: 1960, 1916 cm<sup>-1</sup>

[1H]<sup>3+</sup>: 2062, 1991 cm<sup>-1</sup>

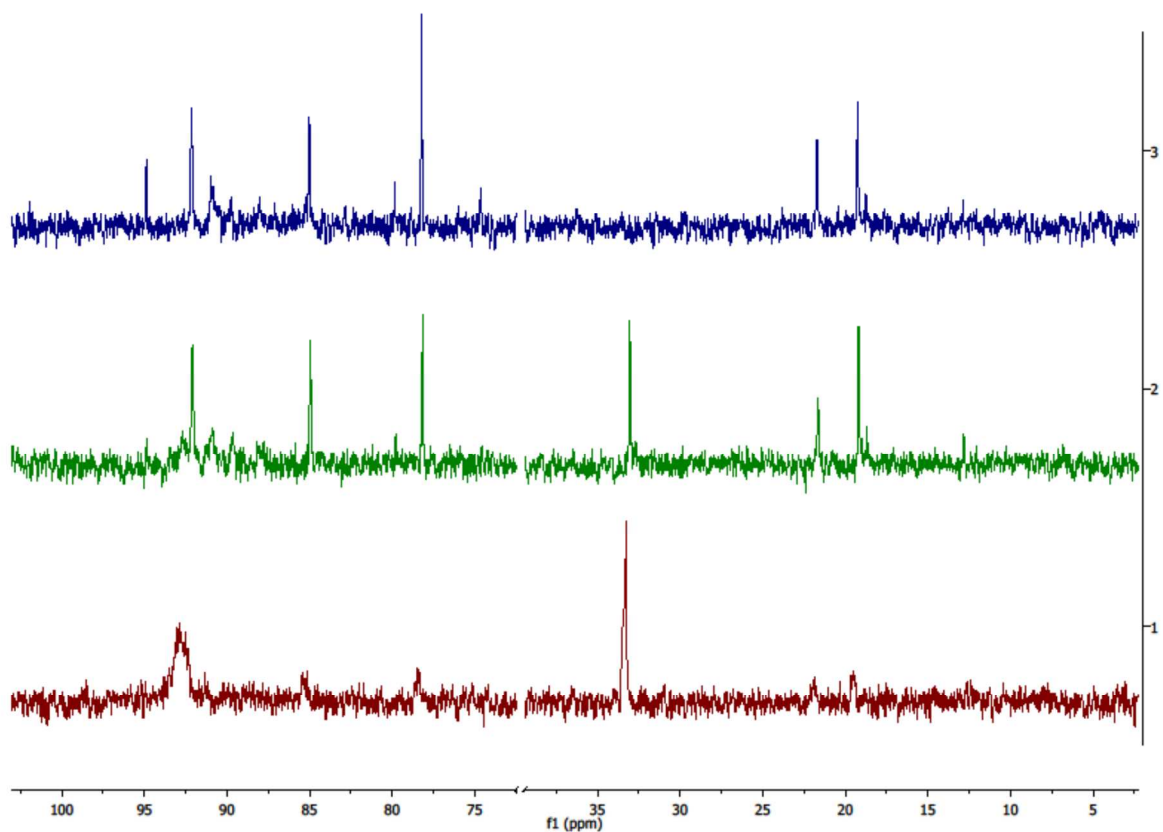


**Figure S31.**  $^{31}\text{P}\{^1\text{H}\}$  NMR spectra of various stages in the reaction of  $\text{Fe}_2(\text{adt}^{\text{Bn}})(\text{CO})_3(\text{dppv})(\text{PMe}_3)$  and 5 equiv of  $[\text{H}(\text{OEt}_2)_2]\text{BAr}^{\text{F}}_4$ : 50 min (bottom, red) and 260 min (middle, green) and 18.25 h (top, blue). The solution was maintained at  $0^\circ\text{C}$  for the first 3 h before being allowed to warm to room temperature overnight.

*Assignments:*

$\text{Fe}_2(\text{adt}^{\text{Bn}})(\text{CO})_3(\text{dppv})(\text{PMe}_3)$ :  $\delta$  92.6, 19.7

$[(\mu\text{-H})\text{Fe}_2(\text{adt}^{\text{Bn}})(\text{CO})_3(\text{dppv})(\text{PMe}_3)]^+$ :  $\delta$  93 and 24.<sup>1</sup>

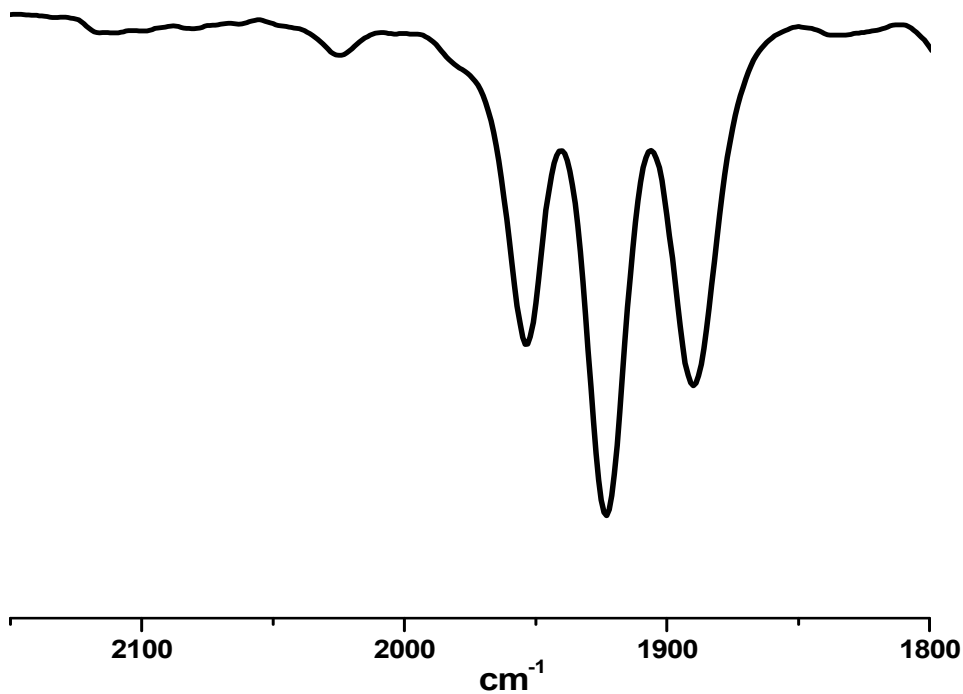


**Figure S32.** IR spectrum resulting from treating  $[1]^0$  with 5 equiv of  $\text{Fc}^*$  and 10 equiv of  $[\text{NPh}_2\text{H}_2]\text{BAr}^{\text{F}}_4$ . By gas chromatographic analysis,  $\sim 0.30$  equiv  $\text{H}_2$  was produced. IR was recorded 4.25 hours after acid was added to  $[1]^0$ .

- (1) Olsen, M. T.; Barton, B. E.; Rauchfuss, T. B. *Inorg. Chem.* 2009, 48, 7507.